HHS Public Access

Author manuscript

J Immunol. Author manuscript; available in PMC 2022 May 01.

Published in final edited form as:

J Immunol. 2021 May 01; 206(9): 2233–2245. doi:10.4049/jimmunol.2001347.

moDCs differentiate into Bcl6^{+} mature moDCs to promote cyclic di-GMP vaccine adjuvant-induced memory T_H cells in the lung

Samira Mansouri[*], **Divya S Katikaneni**[*], **Himanshu Gogoi**[*], **Lei Jin**[*]

[*]Division of Pulmonary, Critical Care and Sleep Medicine, Department of Medicine, The University of Florida, Gainesville, Florida, 32610. U.S.A

Abstract

Induction of lung mucosal immune responses is highly desirable for vaccines against respiratory infections. We recently showed that monocyte-derived DCs (moDCs) are responsible for lung IgA induction. However, the DC subset inducing lung memory T_H cells is unknown. Here, using conditional knockout mice and adoptive cell transfer, we found that moDCs are essential for lung mucosal, but are dispensable for systemic vaccine responses. Next, we showed that mucosal adjuvant cyclic di-GMP differentiated lung moDCs into Bcl6^{+} mature moDCs promoting lung memory T_H cells but dispensable for lung IgA production. Mechanistically, soluble TNF mediates the induction of lung Bcl6^{+} moDCs. Our study reveals the functional heterogeneity of lung moDCs during vaccination and paves the way for a moDCs-targeting vaccine strategy to enhance immune responses on lung mucosa.

Introduction

Vaccination is the most cost-effective approach to fight infectious diseases. Approved vaccines mainly elicit antibody-mediated protection and do not generate strong mucosal responses. Vaccines that induce T-cell-mediated protection in lung mucosa would provide major health and economic benefits. Memory T cells include central memory T cells (T_{CM}), effector memory T cells (T_{EM}), and tissue-resident memory T cells (T_{RM}). T_{RM} cells comprise a majority of memory T cells in the lung and play a crucial role in maintaining long-term protective immunity in the lung mucosa (1, 2). Lung T_{RM} cells include CD4^{+} T_{RM} and CD8^{+} T_{RM} cells.

Lung CD4^{+} T_{RM} cells are crucial for protection against influenza virus and *S.pneumoniae* infection (3, 4). Swain's group showed that lung memory CD4^{+} T cells protect against influenza through multiple synergizing mechanisms (5). Memory CD4^{+} T cells can accelerate primary CD8^{+} T cell responses (6), activate innate immune cells to combat infections (7), and secret T_H cytokines (8). The dendritic cell (DC) subset that promotes the induction of lung CD4^{+} T_{RM} cells is unknown.

Corresponding Author: Lei Jin, Ph.D., Phone number: 352-294-8495, Fax number: 352-273-9154, lei.jin@medicine.ufl.edu.

Conflict of Interest. The authors declare that there is no conflict of interest.

Lung T_{RM} cells (both $CD4^+$ and $CD8^+$ T_{RM}) require local antigen presentation (9–12). In contrast, T_{RM} cells in the intestine, genital tract, or skin, do not require tissue antigen recognition (13, 14). Swain's group first reported that $CD4^+$ T cell memory formation depends on the re-engagement of $CD4^+$ T cells with antigen-presenting cells (APCs) at their effector stage ("Signal 4"), day 5–8 of their response (9, 11). Lung $CD8^+$ T_{RM} establishment also requires cognate antigen recognition in the lung (10). It is unclear which lung APCs provide the "Signal 4" for lung $CD4^+$ T_{RM} induction at this stage of vaccination or infection.

As professional APCs, dendritic cells (DCs) comprise developmental and functional diverse populations. Common DC progenitors (CDPs) generate pre-conventional DCs (pre-cDCs) (15). In the lung, pre-cDCs develop into cDC1 and cDC2. cDC1 expresses CD103 while cDC2 expresses CD11b and CD24 but are CD64-negative. cDC1 are specialized in antigen cross-presentation and priming cytotoxic $CD8^+$ T cells (16). cCD2 prime $CD4^+$ T cells and generate T_H responses (17). Circulating monocytes also give rise to lung DCs (18). Upon infection or inhalation of allergens, lung epithelial cells produce chemokines CCL2 that recruit $CCR2^{hi}$ monocytes (19, 20). In the lung, these infiltrating $CCR2^{hi}$ monocytes upregulate MHC II, CD11c and become monocyte-derived DCs (moDCs). moDCs are found virtually in any disease with substantial inflammation (21).

Bonafide moDCs are highly capable of antigen uptake, processing, presentation, and priming $CD4^+$ and $CD8^+$ T cells (21). For example, tumor-infiltrating moDCs prime $CD8^+$ T cells and induce anti-tumor immunity (22). $CCR2^+$ moDCs are critical for T_H17 induction and the development of experimental autoimmune encephalomyelitis (23). During cutaneous *L. major* infection, moDCs could induce T_H1 polarization (20). moDCs were also sufficient to induce T_H2 immunity by high-dose house dust mite (HDM) asthma (24). Last, we recently showed that moDCs induce T_{FH} cells in the lung by mucosal adjuvant cyclic di-GMP (25). Thus, there is a significant degree of plasticity and heterogeneity in moDCs *in vivo*. The underlying mechanism for moDCs plasticity and heterogeneity is unknown (21).

In this report, we study the role of lung moDCs in generating lung mucosal memory T_H cells. We found that moDCs are specifically required for the generation of memory T_H cells in lung mucosa but not in the systemic compartments. Furthermore, we identified a new differentiated moDCs subpopulation expressing the transcriptional factor (transcriptional repressor B-cell CLL/lymphoma 6) Bcl6 that is responsible for memory T_H cells generation in lung mucosa.

Materials and Methods

Mice.

Age- and gender-matched male, female mice (2 – 3 months old) were used for immunization. C57BL/6J, B6.CD45.1(#002014), $Bcl6^{fl/fl}$ (#023727), $CCR2^{-/-}$ (#004999), $RelA^{fl/fl}$ (#024342), *IL-21-VFP(#030295), CD11c*^{cre} (#008068) and $LysM^{cre}$ (#004781) mice were purchased from The Jackson Laboratory. Mice were housed and bred under pathogen-free conditions in the Animal Research Facility at the University of Florida. Cre-negative littermates were used as controls for experiments. All mouse experiments were

performed by the regulations and approval of the Institutional Animal Care and Use Committee at the University of Florida, IACUC number 201909362.

Reagents.

Eα-OVA (ASFEAQGALANIAVDKA-OVA) fusion protein was produced by GeneCust. TNF-IgG2a-Fc fusion proteins were produced by Creative® Biolabs. WT mouse TNF (aa80~235) or mutant mouse TNF ($TNF_{D221N/A223R}$) was fused with the Fc portion of the mouse IgG2A. Following reagents were from Invivogen, endotoxin-free OVA (vac-pova), vaccine-grade CDG (vac-nacdg). Following reagents were from eBioscience, YAE mAb (14-5741-82). The following reagents are from Biosearch Technologies, NP_6CGG (N-5055A).

The following reagents were obtained from Biolegend: APC-Mouse IgG2A (clone: MOPC173, Cat#981906), anti-mouse CD19–PerCP/Cy5.5 (clone: 1D3/CD19, Cat#152405), anti-mouse LAP (TGFβ1) (clone:TW7–16B4, Cat#141407, 141413), anti-mouse CD45.1-APC (clone:A20, Cat#110713), anti-mouse CD69–APC (clone: H1.2F3, Cat#104578), anti-mouse CD80–FITC (clone: 16–10A1, Cat#104705), anti-mouse CD86–APC-Cy7 (clone: GL-1, Cat#105029), anti-mouse Bcl6–APC (clone: 7D1, Cat#358505), anti-mouse Bcl6–PE (clone: IG191E/A8, Cat#648304), anti-mouse CD4-PE/Cy7 (clone: GK1.5, Cat#100422), anti-mouse IL-4-APC (clone: 11B11, Cat#504106), anti-mouse IL-17a-PE (clone: TC11–1810.1, Cat#506903), anti-mouse IL-4–APC (clone: 11B11, Cat#504105), anti-mouse CD45-PercP/Cy5.5 (clone: 30-F11, Cat#103131), anti-mouse MHCII(I-A/I-E)-Brilliant Violet 421 (clone: M5/114.15.2, Cat#107636), anti-mouse MHCII(I-A/I-E)- Alexa Fluor (clone: M5/114.15.2, Cat#107622), anti-mouse CD11c-APC/Cy7 (clone: N418, Cat#117323), anti-mouse/human CD11b- PE/Cy7 (clone: M1/70, Cat#101216), anti-mouse/human CD11b-Brilliant Violet 605 (clone: M1/70, Cat#101237), anti-mouse CD64- PerCP/Cy5.5 (clone: X54–5/7.1, Cat#139307), anti-mouse TNFR2- PE (Clone:TR75–89, Cat#113405), anti-mouse PD1 (Clone: 29F.1A12, Cat#135214, #135223), anti-mouse IL-10–APC (clone: JESS-16E3, Cat#505016), anti-mouse CXCR–APC (clone: L138D7, Cat#145506), anti-mouse CD49A–PE (clone: HMa1, Cat#142604).

Additional reagents were from InVitrogen: anti-mouse IL-12p35–PE (clone: 27537, Cat#MA5–23559), anti-mouse IL-23–FITC (clone: fc23cpg, Cat#53-7023-80); Miltenyi Biotec: anti-mouse TNFR2-APC (Clone: REA228, Cat#130-104-698); R&D Systems: anti-mouse CXCL13 (Cat#AF470), anti-mouse CCL20–APC-Cy7 (clone: 114906, Cat#IC760N); Cell Signaling Technolog: anti-mouse/human pRelB-PE (clone: D41B9, Cat#:13567), anti-mouse pRelA – APC (clone: 93H1, Cat#4887S); eBioscience: anti-IAb- Eα-peptide complex (clone: YAE, Cat#14-5741-82).

The following reagent was obtained through BEI Resources, NIAID, NIH: Streptococcus pneumoniae Family 2, Clade 3 Pneumococcal Surface Protein A (PspA UAB099) with C-Terminal Histidine Tag, Recombinant from Escherichia coli, NR-33179.

Intranasal CDG Immunization.

Groups of mice were intranasally vaccinated with CDG (5μg) adjuvanted antigen (2μg) or antigen alone (26). For intranasal vaccination, animals were anesthetized using isoflurane in

an E-Z Anesthesia system (Euthanex Corp, Palmer, PA). Antigen, with or without CDG was administered in 30μl saline. Sera were collected at the indicated time points after the last immunization. The antigen-specific Abs were determined by ELISA. Secondary Abs used were anti-mouse IgG-HRP (Southern Biotech, 1033– 05), and anti-mouse IgA-HRP (Southern Biotech, 1040–05).To determine Ag-specific T_H response, splenocytes and lung cells from antigen or CDG + antigen immunized mice were stimulated with 5μg/ml antigen for four days in culture. T_H cytokines were measured in the supernatant by ELISA.

Isolation of lung cells.

Cells were isolated from the lung, as previously described (25). The lungs were perfused with ice-cold PBS and removed. Lungs were digested in DMEM containing 200μg/ml DNase I (Roche, 10104159001), 25μg/ml Liberase TM (Roche, 05401119001) at 37°C for 2 hours. Red blood cells were then lysed and a single cell suspension was prepared by filtering through a 70-μm cell strainer.

Intracellular staining.

For transcription factor Bcl6 staining of murine and human cells, cells were fixed and permeabilized with the Foxp3 staining buffer set (eBioscience, cat no 00-5523-00). The intracellular cytokine staining was performed using the Cytofix/Cytoperm™ kit from BD Biosciences (cat#555028). The single lung cell suspension was fixed in Cytofix/perm buffer (BD Biosciences) in the dark for 20min at RT. Fixed cells were then washed and kept in Perm/Wash buffer at 4°C. Golgi-plug was present during every step before fixation.

Mouse monocyte purification and adoptive transfer

Mouse $Ly6C^{hi}$ monocytes were purified from the bone marrow of naïve mice (C57BL/6J or CD45.1) following the protocol according to the manufacturer (Stemcell Technologies, 19861). Mice were intranasally vaccinated with CDG (5μg) and antigen. $Ly6C^{hi}$ monocytes (1.5 million/mouse) were administered intranasally into immunized mice at 30mins, 2hrs, and 4hrs post-immunization.

Flow cytometry.

Single-cell suspensions were stained with fluorescent-dye-conjugated antibodies in PBS containing 2% FBS and 1mM EDTA. Surface stains were performed at 4°C for 20 min. Cells were washed and stained with surface markers. Cells were then fixed and permeabilized (eBioscience, cat no. 00-5523-00) for intracellular cytokine stain. Data were acquired on a BD LSRFortessa and analyzed using the FlowJo software package (FlowJo, LLC). Cell sorting was performed on the BD FACSAriaIII Flow Cytometer and Cell Sorter.

Experimental Design.

Data exclusion was justified when positive or negative control did not work. All experiments will be repeated at least three times. All repeats are biological replications that involve the same experimental procedures on different mice. Experiments comparing different genotypes, adjuvant responses are designed with individual treatments being assigned randomly. Where possible, treatments will be assigned blindly to the experimenter by

another individual in the lab. When comparing samples from different groups, samples from each group will be analyzed in concert, thereby preventing any biases that may arise from analyzing individual treatments on different days

Statistical Analysis.

All data are expressed as means ± SEM. Statistical significance was evaluated using Prism 6.0 software. One-way ANOVA was performed with post hoc Tukey's multiple comparison test, or Student's t-test applied as appropriate for comparisons between groups. A p-value of <0.05 was considered significant.

Results

CCR2$^{-/-}$ mice selectively lose cyclic di-GMP adjuvanticity in lung mucosa

Mucosal immunization with the adjuvant cyclic di-GMP (CDG) elicits protective immunity in the systemic and mucosal compartments (25–30). However, how CDG promotes mucosal immunity is unknown. We set out to define the mechanisms by which CDG targets pulmonary dendritic cells (DCs) to generate lung mucosal immunity. Pulmonary DCs comprise three unique subsets: cDC1, cDC2, and moDCs (Figure 1A). We have previously shown that moDCs promote lung mucosal T follicular helper (T_{FH}) cells and IgA responses (25, 31). To further evaluate the role of moDCs on lung mucosal immunity we used CCR2$^{-/-}$ mice, as CCR2-deficient mice have reduced numbers of moDCs in the lung at a steady-state (Figure 1B). Mice were immunized intranasally (*i.n.*) twice with CDG and the antigen (pneumococcal surface protein A) PspA at 2-week intervals and the immune responses were examined on day 28 (Figure 1C). We found that CCR2$^{-/-}$ mice had unaltered anti-PspA IgG in the serum but lacked anti-PspA IgA in the bronchoalveolar lavage fluid (BALF) (Figure 1D). We then examined memory $T_H1/2/17$ responses in the spleen and lung from immunized CCR2$^{-/-}$ mice by the *ex-vivo* recall. Again, CCR2$^{-/-}$ mice retained memory T helper (T_H) responses in the spleen but not in the lung (Figure 1E, F). Thus, CDG induced lung mucosal adjuvant responses can be uncoupled from systemic responses. moDCs may be specifically needed for promoting adjuvant responses in lung mucosa.

RelA$^{fl/fl}$CD11c^{cre} mice have a selective loss of CDG-induced lung mucosal vaccine responses.

moDC activation is required for efficient CDG-induced immune responses (22). Lung moDCs require the NF-κB transcription factor RelA for optimal moDC activation (Figure S1A) (25). We generated the RelA$^{fl/fl}$CD11c^{cre} mice to examine the role of moDCs activation in CDG adjuvanticity in the lung mucosa. RelA$^{fl/fl}$CD11c^{cre} mice had no antigen-specific IgA in the BALF while maintaining antigen-specific IgG production in the serum (Figure S1B–S1C). Similar to the CCR2$^{-/-}$ mice, RelA$^{fl/fl}$CD11c^{cre} mice did not generate memory T_H responses in the lung, while having normal memory T_H responses in the spleen (Figure S1D–S1E).

moDCs mediate CDG adjuvant-induced lung mucosal vaccine responses

To further establish that moDCs were responsible for the lack of mucosal immune responses, we performed a monocyte adoptive cell transfer experiment. moDCs differentiate from $Ly6C^{hi}$ monocytes (32). We isolated bone marrow $Ly6C^{hi}$ monocytes from C57BL/6J mice and intranasally transferred the cells into $RelA^{fl/fl}CD11c^{cre}$ mice. The recipient $RelA^{fl/fl}CD11c^{cre}$ mice were then immunized with CDG/OVA. On day 14, the recipient $RelA^{fl/fl}CD11c^{cre}$ mice received a second dose of $Ly6C^{hi}$ monocytes from C57BL/6J mice and were subsequently immunized with CDG/OVA (Figure S1F). Lung mucosal immune responses were analyzed on day 28. $RelA^{fl/fl}CD11c^{cre}$ mice that received WT monocytes restored the lung memory T_H responses and IgA production in the BALF (Figure S1G–1H). Together, the data indicate that lung moDCs mediate CDG-induced lung mucosal-specific IgA and memory T_H cells.

CDG induces moDCs differentiation into $Bcl6^+$ moDCs in the lung

How do moDCs promote mucosal IgA and memory T_H responses in the lung but are dispensable in the spleen? We hypothesized that moDCs might differentiate into a lung-specific subpopulation to induce lung mucosal vaccine responses.

We first examined moDCs in the lungs and mediastinal lymph nodes (medLNs) of WT mice following CDG/PspA immunization (Figure 2A). We noticed that on day 14 post-immunization, the lungs contained a population of moDCs that expressed the transcription factor Bcl6 (Figure 2B). This population was unique to the lung as moDCs in the medLNs of CDG-immunized mice did not express Bcl6 (Figure 2C). Bcl6 is upregulated in $CXCR5^+PD1^+$ T_{FH} cell as well as in B cells prior to entry into the germinal center (33, 34). Bcl6 expression in lung moDCs is lower than those observed in lung $Bcl6^+$ B cells and $CXCR5^+PD1^+$ T cells (Figure 2D). Bcl6 controls the chemokine receptor CXCR5 expression. The new $Bcl6^+$ moDCs express $CXCR5^+$ but the expression is lower than those observed in lung $Bcl6^+$ B cells and $CXCR5^+PD1^+$ T cells (Figure 2D).

To confirm that the $Bcl6^+$ moDCs were indeed monocyte-derived, we isolated $Ly6C^{hi}$ monocyte from CD45.1 mice. The monocytes were then intranasally transferred into C57BL/6J mouse. The recipient WT mice were immunized with CDG/PspA (Figure 2E). On day 14 post-immunization, we identified $CD45.1^+$ $Bcl6^+$ moDCs (Figure 2F). Thus, these $Bcl6^+$ moDCs are indeed monocyte-derived. As alveolar macrophages (AMs) are also monocyte-derived, we examined AMs from the BALF of immunized mice. AMs did not express Bcl6 (Figure 2G). Thus, the $Bcl6^+$ monocyte-derived cells were not AMs.

Next, we examined the kinetics of moDCs differentiation in the lung during CDG immunization. The activation of moDCs, indicated by pRelA and CD80 peaked on days 6 and 9 respectively post-immunization (Figure 2H–2I). Intriguingly, $Bcl6^+$ moDCs differentiation had different kinetics from moDCs activation. $Bcl6^+$ moDCs appeared early on day 2 and peaked on day 14, even when moDCs activation was waning (Figure 2J). On day 14 post-immunization, ~40% of lung moDCs expressed Bcl6 (Figure 2J).

Bcl6$^{fl/fl}$LysM^{cre} mice are defective in lung moDCs development and lack CDG-induced lung mucosal vaccine responses

To understand the functional significance of Bcl6 expression in moDCs populations *in vivo*, we generated Bcl6$^{fl/fl}$LysM^{cre} and Bcl6$^{fl/fl}$CD11c^{cre} mice. Bcl6$^{fl/fl}$LysM^{cre} mice delete Bcl6 in myeloid cells. The cDCs population in the Bcl6$^{fl/fl}$LysM^{cre} mice were unaltered (Figure 3A–B). Bcl6$^{fl/fl}$LysM^{cre} mice had expanded lung neutrophils and Ly6C^{hi} monocytes populations (Figure 3C) as previously reported (35). However, Bcl6$^{fl/fl}$LysM^{cre} mice had reduced lung moDCs (Figure 3A–B), similar to the CCR2$^{-/-}$ mice (Figure 1B) suggesting that Bcl6 expression in myeloid cells is crucial for the differentiation of lung moDCs.

Next, Bcl6$^{fl/fl}$LysM^{cre} mice were immunized with two doses of CDG/NP$_6$CGG at 2-week intervals. Immune memory responses were determined on day 120 (Figure 3D). Bcl6$^{fl/fl}$LysM^{cre} mice did not produce IgA in the BALF (Figure 3E) or lung memory T_H responses (Figure 3G). Similar to the CCR2$^{-/-}$ mice, spleen memory T_H responses and serum antigen-specific IgG in Bcl6$^{fl/fl}$LysM^{cre} mice were comparable to the Bcl6$^{fl/fl}$ mice 4 months post-CDG immunization (Figure 3F, 3H).

Bcl6$^{fl/fl}$CD11c^{cre} mice lack lung cDC1 but retain functional cDC2

As monocytes develop into moDCs, the expression of CD11c is increased. To bypass the influence of Bcl6 on lung moDCs development, we generated Bcl6$^{fl/fl}$CD11c^{cre} mice to ablate Bcl6 after moDCs have developed. Different from the Bcl6$^{fl/fl}$LysM^{cre} mice, Bcl6$^{fl/fl}$CD11c^{cre} mice had increased numbers of lung moDCs at steady-state (Figure 4A–4B).

Bcl6$^{fl/fl}$CD11c^{cre} mice will delete Bcl6 gene in CD11c^{+} cells, including conventional DCs and AMs. Watchmaker, P.B., *et al.,* first showed that CD103^{+}/CD8^{+} cDC1, not Sirpα^{+}IRF4^{+} cDC2, from gastronintestinal tract and spleen, specifically express Bcl6 that is important for cDC1 development (36). Later, Zhang, T. *et.al.*, found that Bcl6 protein expression is elevated in peripheral pre-cDCs, especially cDC1 (37). We observed that Bcl6$^{fl/fl}$CD11c^{cre} mice lack cDC1s in the lung (Figure 4A–4B), confirming that Bcl6 expression in DCs is required for lung cDC1 development. The numbers of lung cDC2 also reduced in Bcl6$^{fl/fl}$CD11c^{cre} mice, though was not statistically significant (Figure 4B).

cDC2 are essential for CDG mucosal adjuvanticity while cDC1 are dispensable (25). We examined the function of lung cDC2 in the Bcl6$^{fl/fl}$CD11c^{cre} mice. Mice were treated (*i.n.*) with CDG for 16hrs. Lung cDC2 activation was determined by CD86 and CCR7 expression. CD86 and CCR7 expression on CDG-activated lung cDC2 were comparable between Bcl6$^{fl/fl}$ and Bcl6$^{fl/fl}$CD11c^{cre} mice (Figure 4C–4D). However, cDC2 from the Bcl6$^{fl/fl}$CD11c^{cre} mice had elevated basal CD86 and CCR7 expression (Figure 4C–4D). To further determine the function of cDC2 in Bcl6$^{fl/fl}$CD11c^{cre} mice, we measured CDG adjuvanticity in the systemic compartments. Three months after CDG immunization, Bcl6$^{fl/fl}$CD11c^{cre} mice had unaltered antigen-specific serum IgG (Figure 4E) and memory T_H responses in the spleen (Figure 4F). Intracellular Bcl6 stain confirmed the lack of Bcl6 upregulation in lung moDCs from Bcl6$^{fl/fl}$CD11c^{cre} (Figure 4G). The phenotypes of the conditional Bcl6 mice were summarized in Table1.

CDG adjuvant induces lung IgA responses but not lung memory T_H responses in $Bcl6^{fl/fl}CD11c^{cre}$ mice

Next, $Bcl6^{fl/fl}CD11c^{cre}$ mice were immunized with CDG/PspA and the vaccine responses were examined 14 days later. Unlike $Bcl6^{fl/fl}LysM^{cre}$ mice, the $Bcl6^{fl/fl}CD11c^{cre}$ mice had unaltered lung IgA (Figure 5A). However, $Bcl6^{fl/fl}CD11c^{cre}$ mice did not generate lung memory lung T_H responses (Figure 5B). We examined CD4 tissue-resident (T_{RMs}) cells, as these cells are a unique population of lung-specific memory T cells. $CD4^+$ T_{RMs} were characterized based on the expression of CD69 and CD49a. $Bcl6^{fl/fl}CD11c^{cre}$ mice did not generate $CD4^+$ T_{RMs} compared to the $Bcl6^{f/f}$ mice following immunization (Figure 5C). Thus, CDG induces lung memory T_H responses but not IgA in $Bcl6^{fl/fl}CD11c^{cre}$ mice.

Transfer of WT moDCs restores CDG-induced lung memory T_H responses in $Bcl6^{fl/fl}CD11c^{cre}$ mice.

To further demonstrate that Bcl6 expression in moDCs, not other $CD11c^+$ cells, are responsible for the loss of lung memory T_H responses in $Bcl6^{fl/fl}CD11c^{cre}$ mice, we adoptively transferred WT moDCs into $Bcl6^{fl/fl}CD11c^{cre}$ mice (Figure 5D). We sorted out lung moDCs from a naïve C57BL/6 mouse and intranasally transferred the moDCs into $Bcl6^{fl/fl}CD11c^{cre}$ mice. Recipient $Bcl6^{fl/fl}CD11c^{cre}$ mice were immunized with CDG/NP_6CGG. We examined lung memory T_H responses on day 14 post-immunization. WT moDCs restored memory T_H1 responses and lung $CD4^+$ T_{RM} cells in the immunized $Bcl6^{fl/fl}CD11c^{cre}$ (Figure 5E–5F). Together, the data indicate that Bcl6 expression in moDCs is required for generating lung memory T_H responses, but not IgA.

Differentiated $Bcl6^+$ lung moDCs present antigen, express co-stimulators, and produce T cell promoting cytokines on day 14 post-immunization

To further understand the role of Bcl6 expression in moDCs, we examined the ability of $Bcl6^+$ moDCs to stimulate T cells. We first asked if lung $Bcl6^+$ DCs were able to present antigen at the effector stage (day 14) *in vivo*. We immunized C57BL/6J mice with CDG plus a fusion protein of Eα peptide (aa52–68) with ovalbumin (Eα-OVA) (Figure 6A). The YAE mAb will detect cells that express the Eα peptide on $I\text{-}A^b$ of MHCII. On day 14 post-immunization, $Bcl6^+$ moDCs were able to present the Eα peptide on MHCII (Figure 6B). Furthermore, the YAE^+Bcl6^+ moDCs were activated, marked by CD86 expression (Figure 6B). Thus, $Bcl6^+$ moDCs were mature APCs and were capable of activating T cells.

We next examined the ability of $Bcl6^+$ moDCs to produce T cell-promoting cytokines (the Signal 3). We immunized C57BL/6J mice with CDG/OVA and characterized the moDCs on Day 14. We measured the production of prototypic T_H1 (IL12p70), T_H2 (IL4), and T_H17 (IL23) promoting cytokines by moDCs (Figure 6C–6E). $Bcl6^+$ moDCs were proficient at producing all these cytokines. Besides, $Bcl6^+$ moDCs were capable of producing IL-10 and TGFβ1, two cytokines that are critical for the induction of T_{RMs} (Figure 6F–6G) (38, 39). Together, the data indicate that the lung-specific $Bcl6^+$ moDCs are mature on day 14 post-immunization and may promote T_H responses in the lung.

IL-21 is a major T_{FH}-inducing cytokine. Using an IL-21 reporter mouse, we found that lung moDCs were the main IL-21-producing lung DCs in the lung on day 14 post-immunization

(Figure 6H). However, the IL-21^{+} moDCs were Bcl6^{-} moDCs (Figure 6H). CXCL13 is essential for germinal center formation. We found that on day 14 post-immunization, moDCs produced CXCL13 (Figure 6I). However, most CXCL13^{+} moDCs were Bcl6^{-} moDCs (Figure 6I). Thus, the lung-specific Bcl6^{+} moDCs do not produce IL-21 or CXCL13.

Lung moDCs in Bcl6$^{fl/fl}$CD11c^{cre} mice are defective in generating T_H promoting cytokines and chemokines.

TGFβ1 are critical cytokines for the induction of T_{RMs} (38, 39). We found that on day 14 post-immunization, lung moDCs from immunized Bcl6$^{fl/fl}$CD11c^{cre} mice had decreased production of TGFβ1 (Figure 7A). Lung moDCs from immunized Bcl6$^{fl/fl}$CD11c^{cre} mice also produced less T_H-promoting cytokines IL-12p70, IL-4, and IL-23 (Figure 7B–7D). CCL20 (MIP3A), the CCR6 ligand, recruits lymphocytes and dendritic cells to mucosal lymphoid tissues and is critical for inducing mucosal immune responses (40). We found that CCL20 production by lung moDCs was also reduced in CDG immunized Bcl6$^{fl/fl}$CD11c^{cre} mice on day 14 (Figure 7E). Thus, Bcl6 expression in moDCs is required for the production of T cell promoting cytokines and chemokines.

Lung TNFR2^{+} cDC2 secrete TNF to generate Bcl6^{+} moDCs in the lung

The Bcl6^{+} moDCs produce T_H and T_{RM} promoting cytokines, chemokines and are likely responsible for lung memory T_H responses. How does CDG induce the differentiation of lung Bcl6^{+} moDCs *in vivo*? We previously showed that the lung TNFR2^{+} cDC2 population induced lung memory T_H responses (Figure 8A) (25). Furthermore, moDCs did not take up intranasal administered CDG (25). We hypothesized that the CDG directly activated TNFR2^{+} cDC2, which drives moDCs differentiation into Bcl6^{+} moDCs.

IRF4$^{fl/fl}$CD11c^{cre} mice lack the cDC2 population and do not respond to CDG immunization (25). We performed an adoptive cell transfer to identify whether TNFR2^{+} cDC2 drive moDC differentiation in IRF4$^{fl/fl}$CD11c^{cre} mice. Lung TNFR2^{+} cDC2 were sorted from WT mice and transferred intranasally into IRF4$^{fl/fl}$CD11c^{cre} mice (Figure 8B). Recipient IRF4$^{fl/fl}$CD11c^{cre} mice were immunized with CDG/PspA. moDCs were characterized on Day 14. IRF4$^{fl/fl}$CD11c^{cre} that received no cells did not generate Bcl6^{+} moDCs (Figure 8C). In contrast, IRF4$^{fl/fl}$CD11c^{cre} received WT TNFR2^{+} cDC2 population had lung Bcl6^{+} moDCs (Figure 8C).

How does the lung TNFR2^{+} cDC2 population stimulate the differentiation of Bcl6^{+} moDCs in the lung? We previously discovered that TNF is essential for CDG mucosal adjuvant activity (26). cDC2 is the main source for intranasal CDG-induced lung TNF (25). We hypothesize that TNFR2^{+} cDC2 cells promote the differentiation of Bcl6^{+} moDCs via TNF secretion. Indeed, the intranasal administration of recombinant soluble TNF/PspA induced lung Bcl6^{+} moDCs in C57BL/6J mice on day 14 post-immunization (Figure 8D).

CDG/TNF-Fc (IgG2A) fusion protein promotes the generation of lung Bcl6^{+} moDCs in the IRF4$^{fl/fl}$CD11c^{cre} mice

To demonstrate that lung TNF acts on moDCs directly to promote the differentiation of Bcl6^{+} moDCs, we generated moDCs-targeting TNF fusion proteins. moDCs express the high-affinity FcR, FcγRI, also known as CD64 that is not found on cDCs or lymphocytes (41). FcγRI binds the Fc of IgG2a with the highest affinity ($10^{8}M^{-1}$), more than 1,000-fold higher than its next binding partner IgG2b-Fc(42). Indeed, intranasal administration of APC-conjugated mouse IgG2A was taken up exclusively by CD64^{+} lung cells, including MHC II^{hi} CD64^{+} moDCs (Figure 8E). The CD64^{+} MHC class II$^{low/int}$ macrophages were also targeted. However, macrophages are dispensable for CDG mucosal adjuvanticity *in vivo* (25, 29). We thus generated a fusion protein TNF-Fc (IgG2A) to target TNF to moDCs (Figure 8F).

CDG immunization generates soluble TNF and transmembrane TNF (tmTNF) (25). We fused TNF with the Fc portion of IgG2A to generate TNF-Fc (IgG2A), which represents soluble TNF (sTNF). We also made a TNF$_{D221N/A223R}$-Fc (IgG2A) fusion protein that targets transmembrane TNF (mTNF) to moDCs. The TNF$_{D221N/A223R}$ mutant mimics transmembrane TNF that binds only to TNFR2, not TNFR1 (43).

We used IRF4$^{fl/fl}$CD11c^{cre} as CDG does not generate lung TNF in the IRF4$^{fl/fl}$CD11c^{cre} (25), which facilitates the TNF-Fc (IgG 2A) complement experiment. We immunized IRF4$^{fl/fl}$CD11c^{cre} mice with CDG/NP$_{6}$CGG with tmTNF or sTNF (Figure 8G). On day 14, we examined lung moDCs (Figure 8G). The addition of sTNF, not mTNF, generated Bcl6^{+} and CCL20^{+} moDCs in the lung (Figure 8H). In contrast, the addition of mTNF generated CXCL13^{+} moDCs (Figure 8H). We propose that sTNF directly induces moDCs differentiation into Bcl6^{+} moDCs.

Discussion

moDCs have a universal presence at the site of inflammation and can promote CD4^{+} and CD8^{+} T cell responses *in vivo*. Yet, we know very little about how moDCs achieve this plasticity *in vivo*. Consequently, we have few approaches to control this common and versatile APC population *in vivo* during inflammation. The most exciting discoveries in this report were the identification of Bcl6^{+} moDCs responsible for lung memory T$_{H}$ *in vivo* and a potential method to induce Bcl6^{+} moDC *in vivo*. Indeed, we recently reported that moDCs-targeting TNF fusion proteins enhanced CDG adjuvanticity in 2-year-old mice (44).

We used the mucosal adjuvant CDG system to study moDCs *in vivo*. CDG activates mainly the STING pathway (26) and does not induce lung damage (29). Its simplicity uncouples the lung mucosal vs. systemic, lung memory T$_{H}$ vs. lung IgA vaccine responses, thus facilitates the extraction of the underlying mechanisms. Lung TNF generates Bcl6^{+} moDCs. TNF is a hallmark of inflammation. We propose that Bcl6^{+} moDCs exist at the site of all inflammation and may play a critical role in driving T$_{H}$ cell-mediated inflammatory responses.

The role of Bcl6 in DCs is not well understood. Ohtsuka, *et al.* first reported that conventional DCs in the spleen requires Bcl6 expression for development in total Bcl6 knockout mice (45). However, Watchmaker, P.B *et al.*, showed that Bcl6 was the transcriptional factor specifically controlling cDC1 development in the gut, lymph nodes, and spleen (36). Zhang, T et al. also found that cDC1 have the highest Bcl6 expression (37). Here, we found that the $Bcl6^{f/f}CD11c^{cre}$ mice lack cDC1 in the lung, but retain functional cDC2 confirming that Bcl6 is specifically required for cDC1 differentiation. We also found that $Bcl6^{f/f}LysM^{cre}$ had reduced moDCs similar to the $CCR2^{-/-}$ mice. Future study is needed to understand the mechanism by which Bcl6 controls cDC1 and moDCs differentiation.

How do $Bcl6^{+}$ moDCs promote the induction of lung $CD4^{+}$ memory T cells? Lung $CD4^{+}$ T cell memory formation depends on the re-engagement of $CD4^{+}$ T cells with APC at their effector stage (Signal 4) (9, 11). The lung $Bcl6^{+}$ moDCs are a differentiated moDCs population that appears in the lung after the initial priming and peaked on day 14. We propose that the differentiated $Bcl6^{+}$ moDCs are the long-thought lung APCs that provide the “Signal 4” during the effector stage to induce lung memory $CD4^{+}$ T cells. Indeed, lung $Bcl6^{+}$ moDCs bore antigens and expressed co-activators on day 14 post-immunization.

The recall response is a hallmark of immune memory cells, which establishes antigen-specificity and distinguishes T_H1, T_H2, and T_H17 memory $CD4^{+}$ T cells. We used lung *ex vivo* recall assays to determine the total lung $CD4^{+}$ memory T cells, including memory T_H1, T_H2, and T_H17 cells induced by immunization. We reasoned that though the lung memory T_H responses are mainly from lung $CD4^{+}$ T_{RM} cells, T_{EM} cells or other unknown memory CD4 T cells in the lung may also contribute to the total lung memory T_H responses (46). Furthermore, growing evidence suggests that T_{RM} cells, even at the same tissue site, *e.g.* lung, are heterogeneous (2). Our goal is to generate antigen-specific protection against lung infections for which all memory $CD4^{+}$ T cells in the lung contribute. We believe measuring total lung memory $T_H1/2/17$ cells by *ex vivo* lung recall is a better indicator for the vaccine efficacy in lung mucosa than enumerating total cell numbers of lung $CD69^{+}CD49a^{+}$ CD4 T_{RM} cells.

In summary, moDCs can differentiate into the new $Bcl6^{+}$ lung moDCs to promote memory $CD4^{+}$ T_H cells in the lung mucosa. Targeted activation of moDCs by soluble TNF fusion protein could be a valuable method to enhance vaccine responses in vulnerable populations, *e.g.* the elderly (44).

Supplementary Material

Refer to Web version on PubMed Central for supplementary material.

Acknowledgments

We thank the Center for Immunology and Transplantation at the University of Florida for the assistance.

This work was supported by NIH grants AI110606, AI125999, AI132865 (to L.J.).

Abbreviations.

CDG	cyclic di-GMP
moDCs	monocyte-derived dendritic cells
T_{FH}	Follicular T helper cells
T_{RM}	Tissue-resident memory T cells
Bcl6	transcriptional repressor B-cell CLL/lymphoma
PspA	pneumococcal surface protein A
AM	alveolar macrophage

References

1. Sathaliyawala T, Kubota M, Yudanin N, Turner D, Camp P, Thome JJ, Bickham KL, Lerner H, Goldstein M, Sykes M, Kato T, and Farber DL. 2013. Distribution and compartmentalization of human circulating and tissue-resident memory T cell subsets. Immunity 38: 187–197. [PubMed: 23260195]
2. Mueller SN, and Mackay LK. 2016. Tissue-resident memory T cells: local specialists in immune defence. Nat Rev Immunol 16: 79–89. [PubMed: 26688350]
3. Teijaro JR, Turner D, Pham Q, Wherry EJ, Lefrancois L, and Farber DL. 2011. Cutting edge: Tissue-retentive lung memory CD4 T cells mediate optimal protection to respiratory virus infection. J Immunol 187: 5510–5514. [PubMed: 22058417]
4. Smith NM, Wasserman GA, Coleman FT, Hilliard KL, Yamamoto K, Lipsitz E, Malley R, Dooms H, Jones MR, Quinton LJ, and Mizgerd JP. 2018. Regionally compartmentalized resident memory T cells mediate naturally acquired protection against pneumococcal pneumonia. Mucosal Immunol 11: 220–235. [PubMed: 28513594]
5. McKinstry KK, Strutt TM, Kuang Y, Brown DM, Sell S, Dutton RW, and Swain SL. 2012. Memory CD4+ T cells protect against influenza through multiple synergizing mechanisms. J Clin Invest 122: 2847–2856. [PubMed: 22820287]
6. Krawczyk CM, Shen H, and Pearce EJ. 2007. Memory CD4 T cells enhance primary CD8 T-cell responses. Infect Immun 75: 3556–3560. [PubMed: 17438031]
7. Strutt TM, McKinstry KK, Dibble JP, Winchell C, Kuang Y, Curtis JD, Huston G, Dutton RW, and Swain SL. 2010. Memory CD4+ T cells induce innate responses independently of pathogen. Nat Med 16: 558–564, 551p following 564. [PubMed: 20436484]
8. McKinstry KK, Strutt TM, and Swain SL. 2010. The potential of CD4 T-cell memory. Immunology 130: 1–9. [PubMed: 20331470]
9. Bautista BL, Devarajan P, McKinstry KK, Strutt TM, Vong AM, Jones MC, Kuang Y, Mott D, and Swain SL. 2016. Short-Lived Antigen Recognition but Not Viral Infection at a Defined Checkpoint Programs Effector CD4 T Cells To Become Protective Memory. J Immunol 197: 3936–3949. [PubMed: 27798159]
10. McMaster SR, Wein AN, Dunbar PR, Hayward SL, Cartwright EK, Denning TL, and Kohlmeier JE. 2018. Pulmonary antigen encounter regulates the establishment of tissue-resident CD8 memory T cells in the lung airways and parenchyma. Mucosal Immunol 11: 1071–1078. [PubMed: 29453412]
11. McKinstry KK, Strutt TM, Bautista B, Zhang W, Kuang Y, Cooper AM, and Swain SL. 2014. Effector CD4 T-cell transition to memory requires late cognate interactions that induce autocrine IL-2. Nat Commun 5: 5377. [PubMed: 25369785]
12. Haddadi S, Vaseghi-Shanjani M, Yao Y, Afkhami S, D'Agostino MR, Zganiacz A, Jeyanathan M, and Xing Z. 2019. Mucosal-Pull Induction of Lung-Resident Memory CD8 T Cells in Parenteral

TB Vaccine-Primed Hosts Requires Cognate Antigens and CD4 T Cells. Front Immunol 10: 2075. [PubMed: 31552032]

13. Mackay LK, Stock AT, Ma JZ, Jones CM, Kent SJ, Mueller SN, Heath WR, Carbone FR, and Gebhardt T. 2012. Long-lived epithelial immunity by tissue-resident memory T (TRM) cells in the absence of persisting local antigen presentation. Proc Natl Acad Sci U S A 109: 7037–7042. [PubMed: 22509047]
14. Casey KA, Fraser KA, Schenkel JM, Moran A, Abt MC, Beura LK, Lucas PJ, Artis D, Wherry EJ, Hogquist K, Vezys V, and Masopust D. 2012. Antigen-independent differentiation and maintenance of effector-like resident memory T cells in tissues. J Immunol 188: 4866–4875. [PubMed: 22504644]
15. Onai N, Obata-Onai A, Schmid MA, and Manz MG. 2007. Flt3 in regulation of type I interferon-producing cell and dendritic cell development. Ann N Y Acad Sci 1106: 253–261. [PubMed: 17360795]
16. Desch AN, Randolph GJ, Murphy K, Gautier EL, Kedl RM, Lahoud MH, Caminschi I, Shortman K, Henson PM, and Jakubzick CV. 2011. CD103+ pulmonary dendritic cells preferentially acquire and present apoptotic cell-associated antigen. J Exp Med 208: 1789–1797. [PubMed: 21859845]
17. Beaty SR, Rose CE Jr., and Sung SS. 2007. Diverse and potent chemokine production by lung CD11bhigh dendritic cells in homeostasis and in allergic lung inflammation. J Immunol 178: 1882–1895. [PubMed: 17237439]
18. Jakubzick C, Tacke F, Ginhoux F, Wagers AJ, van Rooijen N, Mack M, Merad M, and Randolph GJ. 2008. Blood monocyte subsets differentially give rise to CD103+ and CD103- pulmonary dendritic cell populations. J Immunol 180: 3019–3027. [PubMed: 18292524]
19. Hammad H, Chieppa M, Perros F, Willart MA, Germain RN, and Lambrecht BN. 2009. House dust mite allergen induces asthma via Toll-like receptor 4 triggering of airway structural cells. Nat Med 15: 410–416. [PubMed: 19330007]
20. Leon B, Lopez-Bravo M, and Ardavin C. 2007. Monocyte-derived dendritic cells formed at the infection site control the induction of protective T helper 1 responses against Leishmania. Immunity 26: 519–531. [PubMed: 17412618]
21. Chow KV, Sutherland RM, Zhan Y, and Lew AM. 2017. Heterogeneity, functional specialization and differentiation of monocyte-derived dendritic cells. Immunol Cell Biol 95: 244–251. [PubMed: 27748730]
22. Sharma MD, Rodriguez PC, Koehn BH, Baban B, Cui Y, Guo G, Shimoda M, Pacholczyk R, Shi H, Lee EJ, Xu H, Johnson TS, He Y, Mergoub T, Venable C, Bronte V, Wolchok JD, Blazar BR, and Munn DH. 2018. Activation of p53 in Immature Myeloid Precursor Cells Controls Differentiation into Ly6c(+)CD103(+) Monocytic Antigen-Presenting Cells in Tumors. Immunity 48: 91–106 e106. [PubMed: 29343444]
23. Ko HJ, Brady JL, Ryg-Cornejo V, Hansen DS, Vremec D, Shortman K, Zhan Y, and Lew AM. 2014. GM-CSF-responsive monocyte-derived dendritic cells are pivotal in Th17 pathogenesis. J Immunol 192: 2202–2209. [PubMed: 24489100]
24. Plantinga M, Guilliams M, Vanheerswynghels M, Deswarte K, Branco-Madeira F, Toussaint W, Vanhoutte L, Neyt K, Killeen N, Malissen B, Hammad H, and Lambrecht BN. 2013. Conventional and monocyte-derived CD11b(+) dendritic cells initiate and maintain T helper 2 cell-mediated immunity to house dust mite allergen. Immunity 38: 322–335. [PubMed: 23352232]
25. Mansouri S, Patel S, Katikaneni DS, Blaauboer SM, Wang W, Schattgen S, Fitzgerald K, and Jin L. 2019. Immature lung TNFR2(−) conventional DC 2 subpopulation activates moDCs to promote cyclic di-GMP mucosal adjuvant responses in vivo. Mucosal Immunol 12: 277–289. [PubMed: 30327534]
26. Blaauboer SM, Gabrielle VD, and Jin L. 2014. MPYS/STING-mediated TNF-alpha, not type I IFN, is essential for the mucosal adjuvant activity of (3'−5')-cyclic-di-guanosine-monophosphate in vivo. J Immunol 192: 492–502. [PubMed: 24307739]
27. Ebensen T, Schulze K, Riese P, Link C, Morr M, and Guzman CA. 2007. The bacterial second messenger cyclic diGMP exhibits potent adjuvant properties. Vaccine 25: 1464–1469. [PubMed: 17187906]

28. Allen AC, Wilk MM, Misiak A, Borkner L, Murphy D, and Mills KHG. 2018. Sustained protective immunity against Bordetella pertussis nasal colonization by intranasal immunization with a vaccine-adjuvant combination that induces IL-17-secreting TRM cells. Mucosal Immunol 11: 1763–1776. [PubMed: 30127384]
29. Blaauboer SM, Mansouri S, Tucker HR, Wang HL, Gabrielle VD, and Jin L. 2015. The mucosal adjuvant cyclic di-GMP enhances antigen uptake and selectively activates pinocytosis-efficient cells in vivo. Elife 4.
30. Gogoi H, Mansouri S, and Jin L. 2020. The Age of Cyclic Dinucleotide Vaccine Adjuvants. Vaccines (Basel) 8.
31. Richmond BW, Mansouri S, Serezani A, Novitskiy S, Blackburn JB, Du RH, Fuseini H, Gutor S, Han W, Schaff J, Vasiukov G, Xin MK, Newcomb DC, Jin L, Blackwell TS, and Polosukhin VV. 2020. Monocyte-derived dendritic cells link localized secretory IgA deficiency to adaptive immune activation in COPD. Mucosal Immunol.
32. Randolph GJ, Beaulieu S, Lebecque S, Steinman RM, and Muller WA. 1998. Differentiation of monocytes into dendritic cells in a model of transendothelial trafficking. Science 282: 480–483. [PubMed: 9774276]
33. Kitano M, Moriyama S, Ando Y, Hikida M, Mori Y, Kurosaki T, and Okada T. 2011. Bcl6 protein expression shapes pre-germinal center B cell dynamics and follicular helper T cell heterogeneity. Immunity 34: 961–972. [PubMed: 21636294]
34. Denton AE, Innocentin S, Carr EJ, Bradford BM, Lafouresse F, Mabbott NA, Morbe U, Ludewig B, Groom JR, Good-Jacobson KL, and Linterman MA. 2019. Type I interferon induces CXCL13 to support ectopic germinal center formation. J Exp Med 216: 621–637. [PubMed: 30723095]
35. Zhu B, Zhang R, Li C, Jiang L, Xiang M, Ye Z, Kita H, Melnick AM, Dent AL, and Sun J. 2019. BCL6 modulates tissue neutrophil survival and exacerbates pulmonary inflammation following influenza virus infection. Proc Natl Acad Sci U S A 116: 11888–11893. [PubMed: 31138703]
36. Watchmaker PB, Lahl K, Lee M, Baumjohann D, Morton J, Kim SJ, Zeng R, Dent A, Ansel KM, Diamond B, Hadeiba H, and Butcher EC. 2014. Comparative transcriptional and functional profiling defines conserved programs of intestinal DC differentiation in humans and mice. Nat Immunol 15: 98–108. [PubMed: 24292363]
37. Zhang TT, Liu D, Calabro S, Eisenbarth SC, Cattoretti G, and Haberman AM. 2014. Dynamic expression of BCL6 in murine conventional dendritic cells during in vivo development and activation. PLoS One 9: e101208. [PubMed: 24979752]
38. Thompson EA, Darrah PA, Foulds KE, Hoffer E, Caffrey-Carr A, Norenstedt S, Perbeck L, Seder RA, Kedl RM, and Lore K. 2019. Monocytes Acquire the Ability to Prime Tissue-Resident T Cells via IL-10-Mediated TGF-beta Release. Cell Rep 28: 1127–1135 e1124. [PubMed: 31365858]
39. Nath AP, Braun A, Ritchie SC, Carbone FR, Mackay LK, Gebhardt T, and Inouye M. 2019. Comparative analysis reveals a role for TGF-beta in shaping the residency-related transcriptional signature in tissue-resident memory CD8+ T cells. PLoS One 14: e0210495. [PubMed: 30742629]
40. Lee AYS, and Korner H. 2019. The CCR6-CCL20 axis in humoral immunity and T-B cell immunobiology. Immunobiology 224: 449–454. [PubMed: 30772094]
41. Langlet C, Tamoutounour S, Henri S, Luche H, Ardouin L, Gregoire C, Malissen B, and Guilliams M. 2012. CD64 expression distinguishes monocyte-derived and conventional dendritic cells and reveals their distinct role during intramuscular immunization. J Immunol 188: 1751–1760. [PubMed: 22262658]
42. Guilliams M, Bruhns P, Saeys Y, Hammad H, and Lambrecht BN. 2014. The function of Fcgamma receptors in dendritic cells and macrophages. Nat Rev Immunol 14: 94–108. [PubMed: 24445665]
43. Loetscher H, Stueber D, Banner D, Mackay F, and Lesslauer W. 1993. Human tumor necrosis factor alpha (TNF alpha) mutants with exclusive specificity for the 55-kDa or 75-kDa TNF receptors. J Biol Chem 268: 26350–26357. [PubMed: 8253759]
44. Gogoi H, Mansouri S, Katikaneni DS, and Jin L. 2020. New MoDC-Targeting TNF Fusion Proteins Enhance Cyclic Di-GMP Vaccine Adjuvanticity in Middle-Aged and Aged Mice. Front Immunol 11: 1674. [PubMed: 32849581]

45. Ohtsuka H, Sakamoto A, Pan J, Inage S, Horigome S, Ichii H, Arima M, Hatano M, Okada S, and Tokuhisa T. 2011. Bcl6 is required for the development of mouse CD4+ and CD8alpha+ dendritic cells. J Immunol 186: 255–263. [PubMed: 21131418]

46. Reagin KL, and Klonowski KD. 2018. Incomplete Memories: The Natural Suppression of Tissue-Resident Memory CD8 T Cells in the Lung. Front Immunol 9: 17. [PubMed: 29403499]

Key points:

- moDCs mediate CDG-induced lung mucosal, not systematic, vaccine responses.
- CDG induces a new $Bcl6^+$ moDCs population that promotes lung memory T_H responses.
- TNF induces the generation of lung $Bcl6^+$ moDCs.

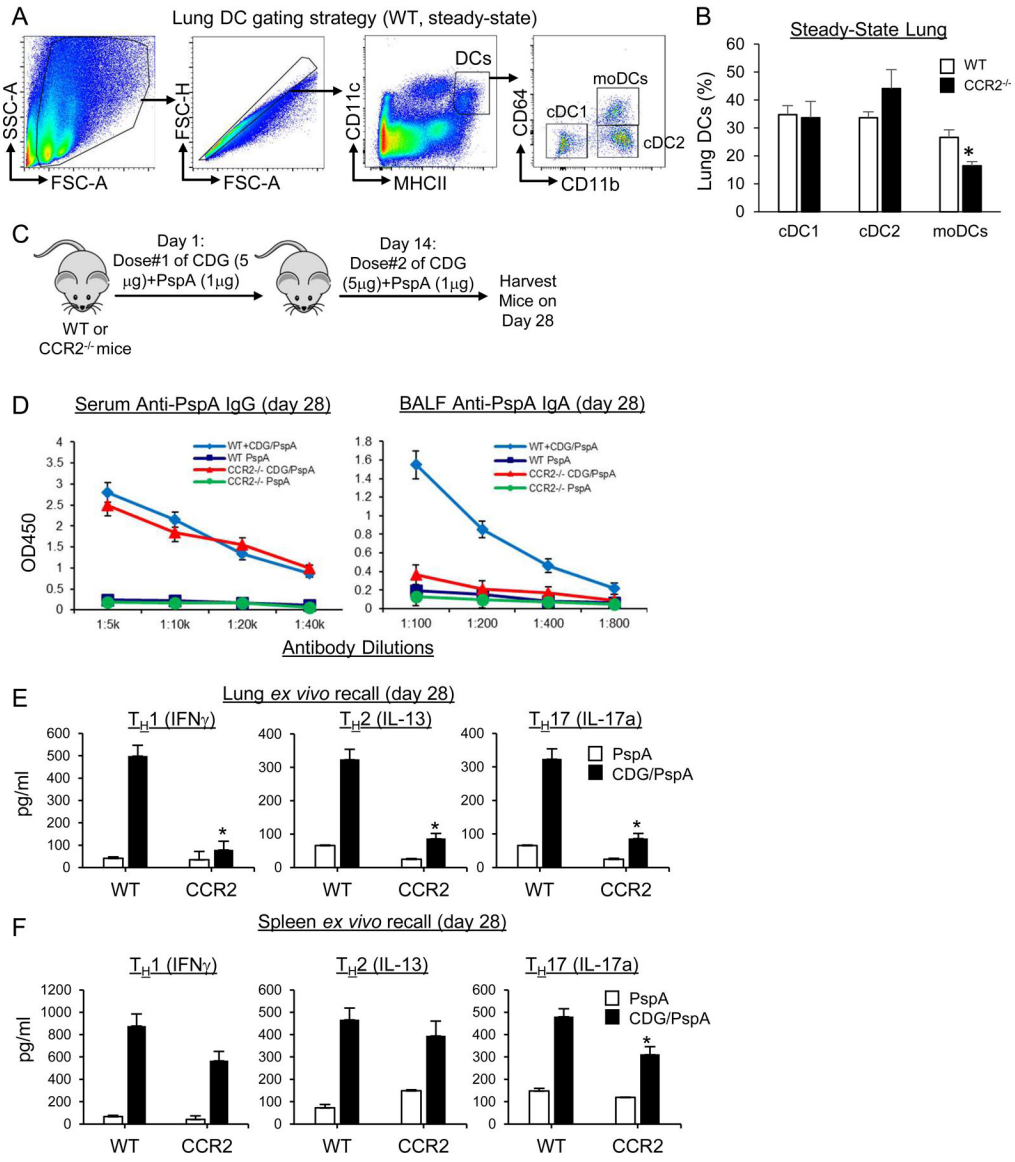

Figure 1. CCR2$^{-/-}$ mice selectively lose CDG adjuvant responses in lung mucosa but not in the systemic compartments.

A. Gating strategy for lung DCs. Lung cDC1 are gated as MHCII^{hi}CD11c^{+}CD11b^{-}CD64^{-}, moDCs are MHCII^{hi}CD11c^{+}CD11b^{+}CD64^{+}, and cDC2 are MHCII^{hi}CD11c^{+}CD11b^{+}CD64^{-}. **B.** Frequency of lung DCs at steady-state in WT and CCR2$^{-/-}$ mice (n=3mice/group). Data are representative of four independent experiments. **C.** Experimental design for the immunization of WT and CCR2$^{-/-}$ mice. Mice were immunized intranasally (*i.n.*) with two doses of PspA (1μg) or PspA (1μg) plus CDG (5μg) at two-week intervals. **D.** Anti-PspA IgG in serum (left) and IgA in BALF (right) were determined by ELISA 28 days post-immunization (n=3mice/group). Data are representative of three independent experiments. **E-F.** Lung cells (**E**) or splenocytes (**F**) from immunized mice were stimulated with 5μg/ml PspA for 4 days in culture. Cytokines were measured in the supernatant by ELISA. Data are representative of three independent experiments. Graphs represent the mean with error bars

indication s.e.m. *P* values determined by unpaired student *t*-test (**B**) or one-way ANOVA Tukey's multiple comparison test (**E, F**). *$P<0.05$

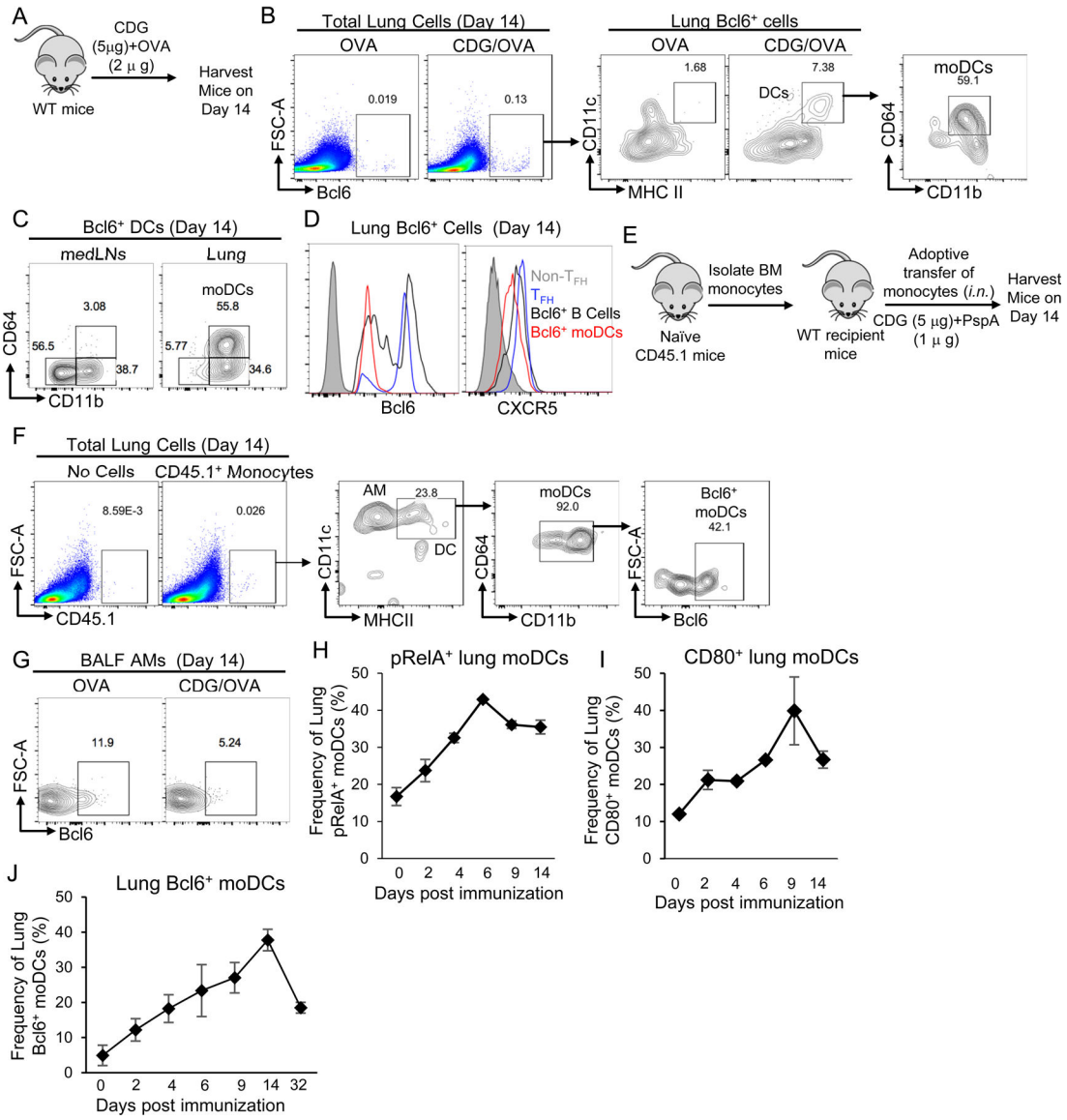

Figure 2. moDCs differentiate into lung-specific Bcl6$^+$ moDCs on day 14 post CDG immunization.

A. Experimental design for moDC characterization. C57BL/6 mice were immunized intranasally with CDG (5μg) and OVA (2μg). Lung moDCs were characterized by flow cytometry on day 14. **B.** Flow cytometry analysis of Bcl6 expressing cells in the lung of mice immunized with CDG/OVA as in **A** on day 14. (n=3mice/group). Data are representative of two independent experiments. **C.** Flow cytometry analysis of Bcl6 expressing DCs in the mediastinal lymph nodes (medLNs) and lungs of WT mice immunized with CDG/OVA as in **A**. Lungs were harvested on day 14. Data are representative of two independent experiments. **D.** Bcl6 and CXCR5 expression on indicated cell populations in the lung of C57BL/6J mice on day 14 post CDG/NP$_6$CGG immunization. Non-T$_{FH}$ cells were gated as CD4$^+$CXCR5$^-$PD1$^-$. T$_{FH}$ cells were gated as CD4$^+$CXCR5$^+$PD1$^+$. Bcl6$^+$ B cells were gated as CD19$^+$Bcl6$^+$ (n=3mice/group). Data are representative of three independent experiments. **E.** Experimental design for monocyte

adoptive transfer. Ly6c^{hi} monocytes were isolated from the bone marrow of CD45.1 mice. CD45.1^{+} monocytes (1.5 million cells) were intranasally transferred into C57BL/6J mice. Recipient WT mice were immunized with CDG (5μg) and PspA (1μg). Mice were harvested on day 14. **F.** Flow cytometry analysis of CD45.1^{+} cells following monocyte adoptive transfer. On day 14, CD45.1^{+}Bcl6^{+} moDCs were determined by Flow cytometry. (n=3mice/group). Data are representative of two independent experiments. **G.** Flow cytometry analysis of Bcl6 expression in alveolar macrophages in the BALF of WT mice on day 14 post CDG/OVA immunization (n=3mice/group). Data are representative of three independent experiments. **H-J.** Flow cytometry analysis of the kinetics of pRelA^{+} (**H**), CD80^{+} (**I**), and Bcl6^{+} moDCs (**J**) from WT mice immunized with CDG (5μg) and OVA (2μg). Lungs were harvested at different time points (n=3mice/group). Data are representative of two independent experiments.

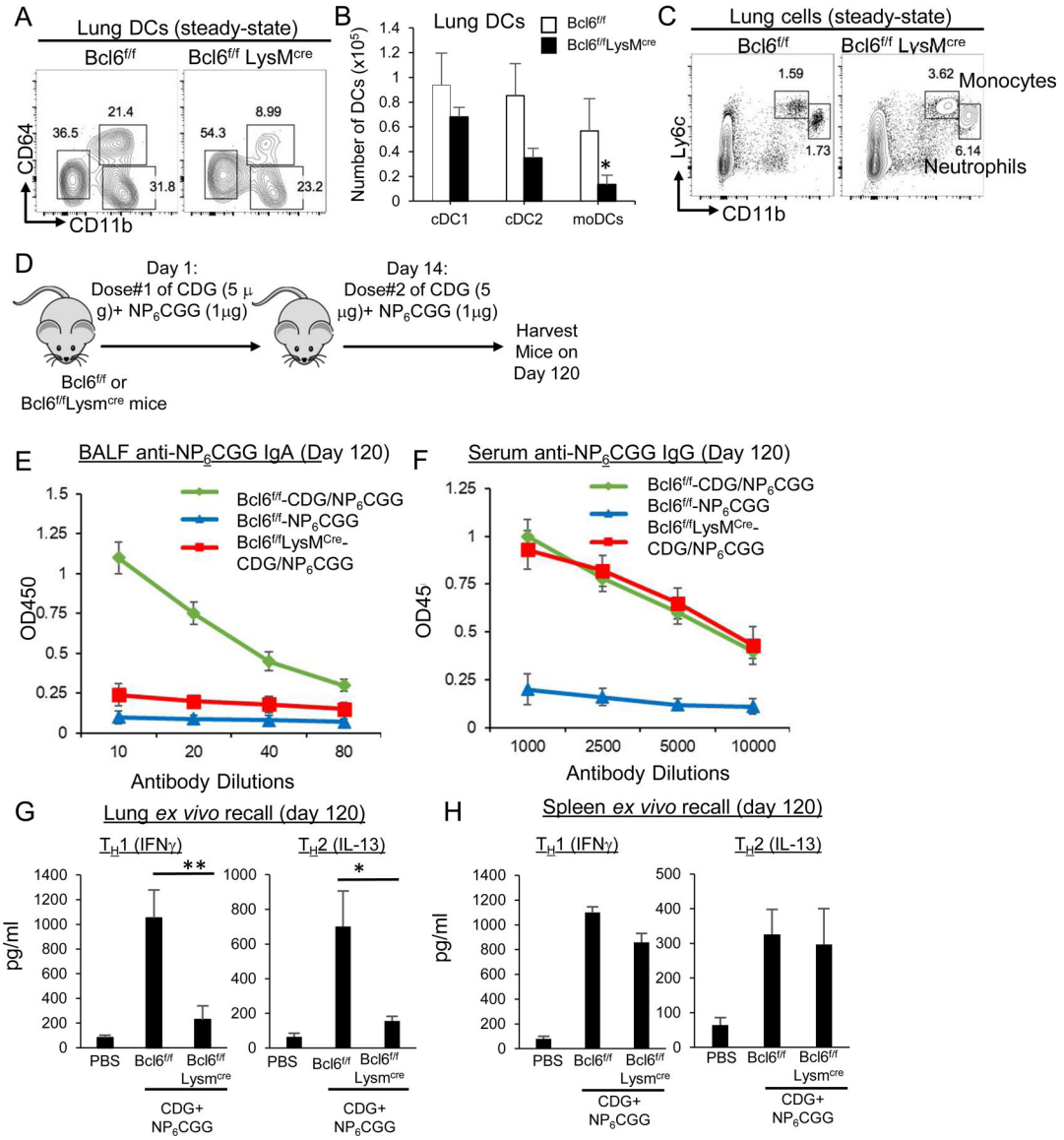

Figure 3. Bcl6 expression in LysM^{+} cells is required for lung moDCs development.

A-B. Flow cytometry analysis (**A**) and absolute number (**B**) of pulmonary DCs subsets in Bcl6$^{fl/fl}$ and Bcl6$^{fl/fl}$LysM^{cre} mice at steady-state (n=3 mice/group). Data are representative of two independent experiments. **C.** Flow cytometry analysis lung Ly6C^{hi} monocytes and neutrophils in Bcl6$^{fl/fl}$ and Bcl6$^{fl/fl}$LysM^{cre} mice at steady-state (n=3 mice/group). Data are representative of two independent experiments. **D.** Experimental design for the immunization of Bcl6$^{fl/fl}$ and Bcl6$^{fl/fl}$LysM^{cre} mice. Mice were immunized intranasally (*i.n.*) with two doses of NP_6CGG (1µg) or NP_6CGG (1µg) plus CDG (5µg) at two-week intervals. Mice were then harvested on day 120 post-immunization. **E-F.** Anti-NP_6CGG IgG in serum (**E**) and BALF IgA (**F**) were determined by ELISA on day 120 post-immunization. (n=3 mice/group) Data are representative of three independent experiments. **G-H.** Lung cells (**G**) and splenocytes (**H**) from immunized Bcl6$^{fl/fl}$ and Bcl6$^{fl/fl}$LysM^{cre} mice were recalled with 5µg/ml NP_6CGG for 4 days in culture. Cytokines were measured in the supernatant by

ELISA. Data are representative of three independent experiments (n=3 mice/group). Graphs represent the mean with error bars indication s.e.m. The significance is determined by one-way ANOVA Tukey's multiple comparison test (**G**) or unpaired Student's t-test (**B**). *p<0.05, ***P*<0.001.

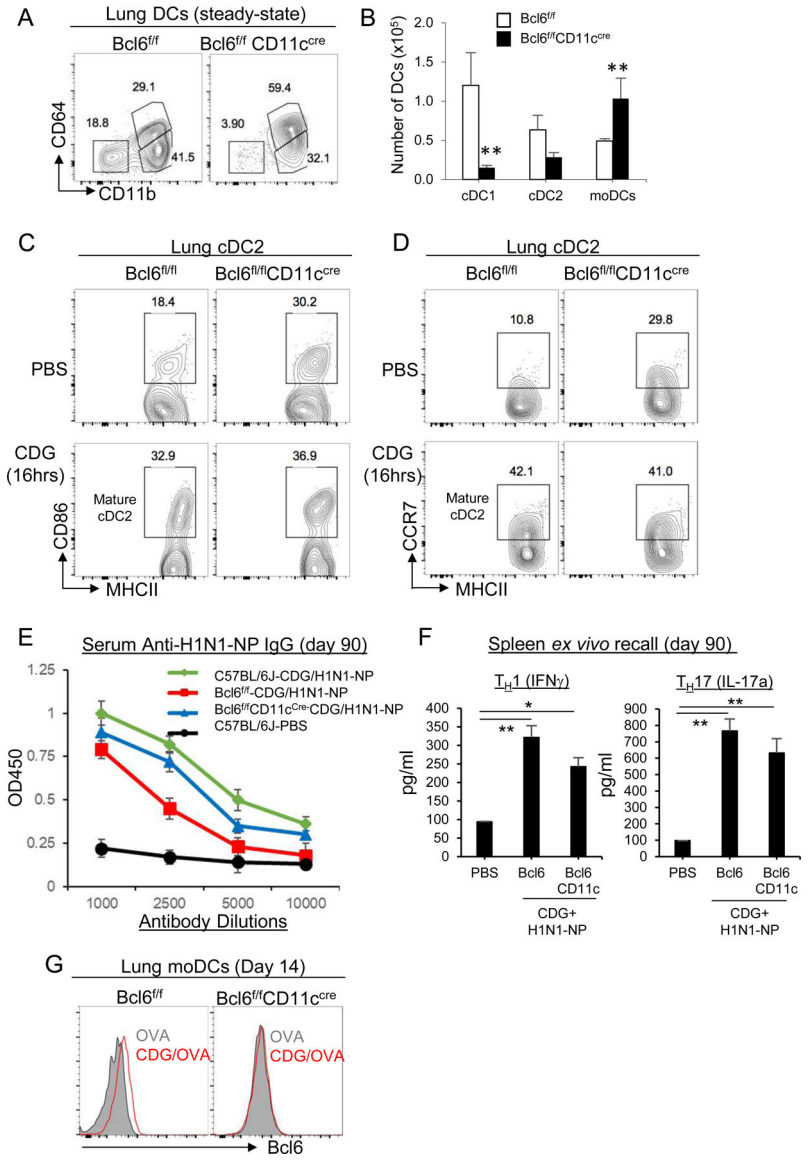

Figure 4. Bcl6 expression in CD11c^{+} cells is dispensable for CDG-induced systemic vaccine responses.

A-B. Flow cytometry analysis (**A**) and absolute number (**B**) of pulmonary DCs subsets in Bcl6$^{fl/fl}$ and Bcl6$^{fl/fl}$CD11c^{cre} mice at steady-state (n=3mice/group). Data are representative of three independent experiments. **C-D.** Bcl6$^{fl/fl}$ and Bcl6$^{fl/fl}$CD11c^{cre} mice were intranasally treated with CDG (5μg) or PBS for 16hrs. CD86 and CCR7 expression on lung cDC2 were determined by flow cytometry. (n=3mice/group). Data are representative of two independent experiments. **E.** Bcl6$^{fl/fl}$ and Bcl6$^{fl/fl}$CD11c^{cre} mice were immunized (*i.n.*) with CDG/H1N1-NP twice at the two-week interval. Serum anti-H1N1-NP IgG was determined by ELISA on day 90 post-immunization (n=3mice/group). Data are representative of two independent experiments. **F.** Lung cells from immunized Bcl6$^{fl/fl}$ and Bcl6$^{fl/fl}$CD11c^{cre} mice were recalled with 5μg/ml H1N1-NP for 4 days in culture. Cytokines were measured in the supernatant by ELISA. Data are representative of two independent experiments. **G**. Bcl6$^{fl/fl}$ and Bcl6$^{fl/fl}$CD11c^{cre} mice were immunized (*i.n.*) with CDG/OVA or OVA. Bcl6 expression

in lung moDCs were determined by flow cytometry. (n=3mice/group). Data are representative of two independent experiments. Graphs represent mean ± standard error. The significance is determined by unpaired Student's t-test (**B**) or one-way ANOVA Tukey's multiple comparisons (**F**). *p<0.05, ***P*<0.001.

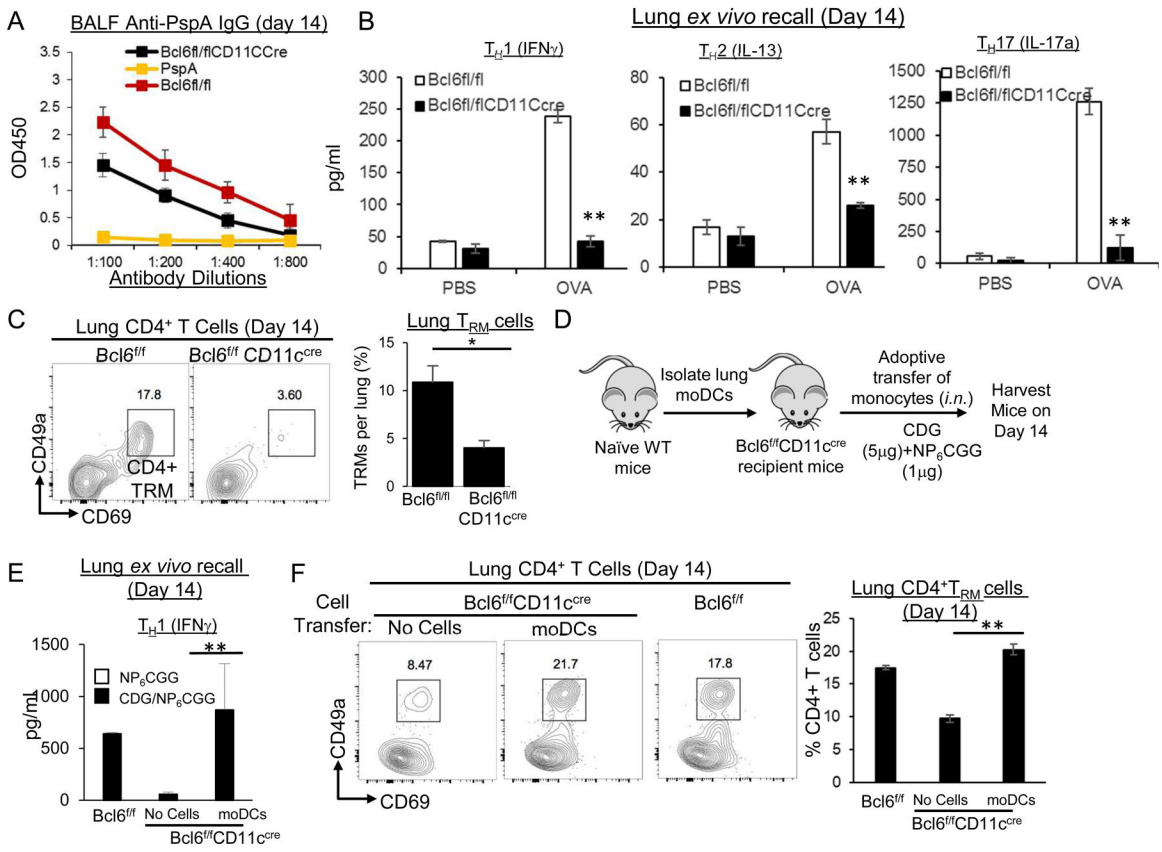

Figure 5. Bcl6 expression in moDCs is specifically required for CDG-induced lung memory T_H response.

A. $Bcl6^{fl/fl}$ and $Bcl6^{fl/fl}CD11c^{cre}$ mice were immunized (*i.n.*) with CDG (5μg) and PspA (2μg). BALF anti-PspA IgA was determined on day 14 by ELISA. (n=3 mice/group). Data are representative of three independent experiments. **B.** Lung cells from immunized mice (**A**) were recalled with 5μg/ml PspA for 4 days in culture. Cytokines were measured in the supernatant by ELISA. Data are representative of three independent experiments. **C.** Flow cytometry plots (left) and frequency (right) of $CD4^+CD69^+CD49a^+$ T_{RM} in immunized $Bcl6^{fl/fl}$ and $Bcl6^{fl/fl}CD11c^{cre}$ mice from (**A**). Data are representative of three independent experiments. **D.** Experimental design for moDC adoptive transfer. moDCs were isolated from the lungs of naïve WT mice. moDCs were (~35,000 cells) were intranasally transferred into $Bcl6^{fl/fl}CD11c^{cre}$ mice. Recipient $Bcl6^{fl/fl}CD11c^{cre}$ mice were immunized with CDG (5μg) and NP_6CGG (1μg). Mice were harvested on day 14. **E.** Lung cells from immunized mice (**D**) were recalled with 5μg/ml NP_6CGG for 4 days in culture. Cytokines were measured in the supernatant by ELISA (n=3mice/group). **F.** Flow cytometry analysis (left) and frequency (right) of $CD4^+CD69^+CD49a^+$ T_{RM} following adoptive transfer in **E**. Data are representative of two independent experiments. Graphs represent means ± s.e.m. The significance is determined by unpaired Student's t-test (**B**, **C**) or one-way ANOVA Tukey's multiple comparison test (**E, F**). *p<0.05, ***P*<0.001.

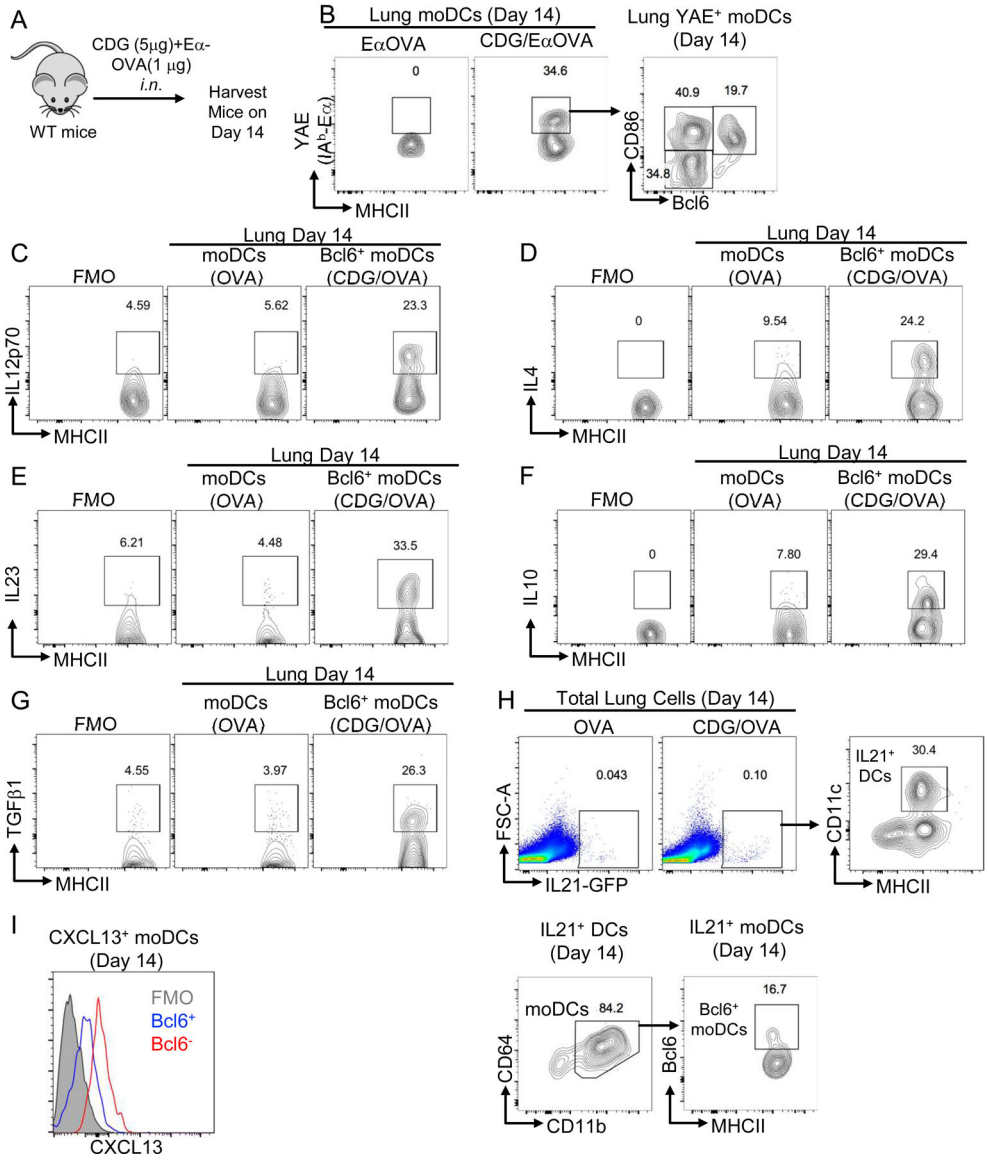

Figure 6. Lung Bcl6^{+} moDCs are mature DCs producing T-cell promoting cytokines on day 14 post CDG immunization.

A. Experimental design for moDC characterization. C57BL/6 mice were immunized intranasally with CDG (5μg) and Eα-OVA (1μg). Control C57BL/6 mice were immunized intranasally with Eα-OVA (1μg). Lung moDCs were characterized by flow cytometry on day 14. **B.** WT mice were immunized with Eα-OVA or Eα-OVA/CDG (5μg). Cells that presented Eα on I-A^{b} of MHCII were determined with the YAE mAb by flow cytometry in the lung on day 14. (n=3mice/group). Data are representative of three independent experiments. **C-G.** Flow cytometry analysis of IL12p70 (**C**), IL4 (**D**), IL23 (**E**) IL10 (**F**), and TGFβ1 (**G**) production by lung moDCs in C57BL/6J mice on day 14 post-CDG/OVA immunization (n=3mice/group). Data are representative of two independent experiments. **H.** Analysis of IL-21^{+} cells in the lungs of IL-21-VFP reporter mice on day 14 post-immunization with CDG/OVA (*i.n.*) (n=3mice/group). Data are representative of two independent experiments. **I.** Flow cytometry analysis of CXCL13^{+} lung moDCs in

C57BL/6J mice on day 14 post-immunization (*i.n.*) with CDG/OVA (n=3mice/group). Data are representative of two independent experiments.

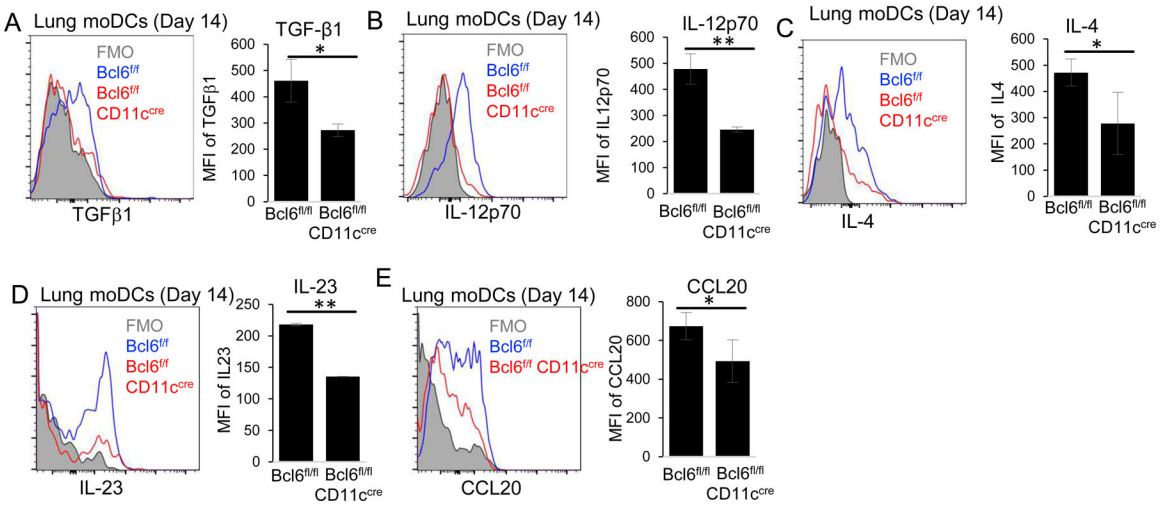

Figure 7. Lung moDCs in Bcl6$^{fl/fl}$CD11c^{cre} mice are defective in producing T_H cell polarizing cytokines and chemokines.

A-E. Bcl6$^{fl/fl}$ and Bcl6$^{fl/fl}$CD11c^{cre} mice were immunized (*i.n.*) with CDG (5μg) and NP_6CGG (1μg). Mice were harvested on day 14. Flow cytometry analysis and frequency of TGFβ1 (**A**), IL-12p70 (**B**), IL-4 (**C**), IL-23 (**D**), and CCL20 (**E**) production by lung moDCs from Bcl6$^{fl/fl}$ and Bcl6$^{fl/fl}$CD11c^{cre} mice on day 14 post CDG/NP_6CGG immunization (n=3mice/group). Data are representative of two independent experiments. Graphs represent mean ± standard error. The significance is determined by the unpaired Student's t-test. * $p<0.05$.

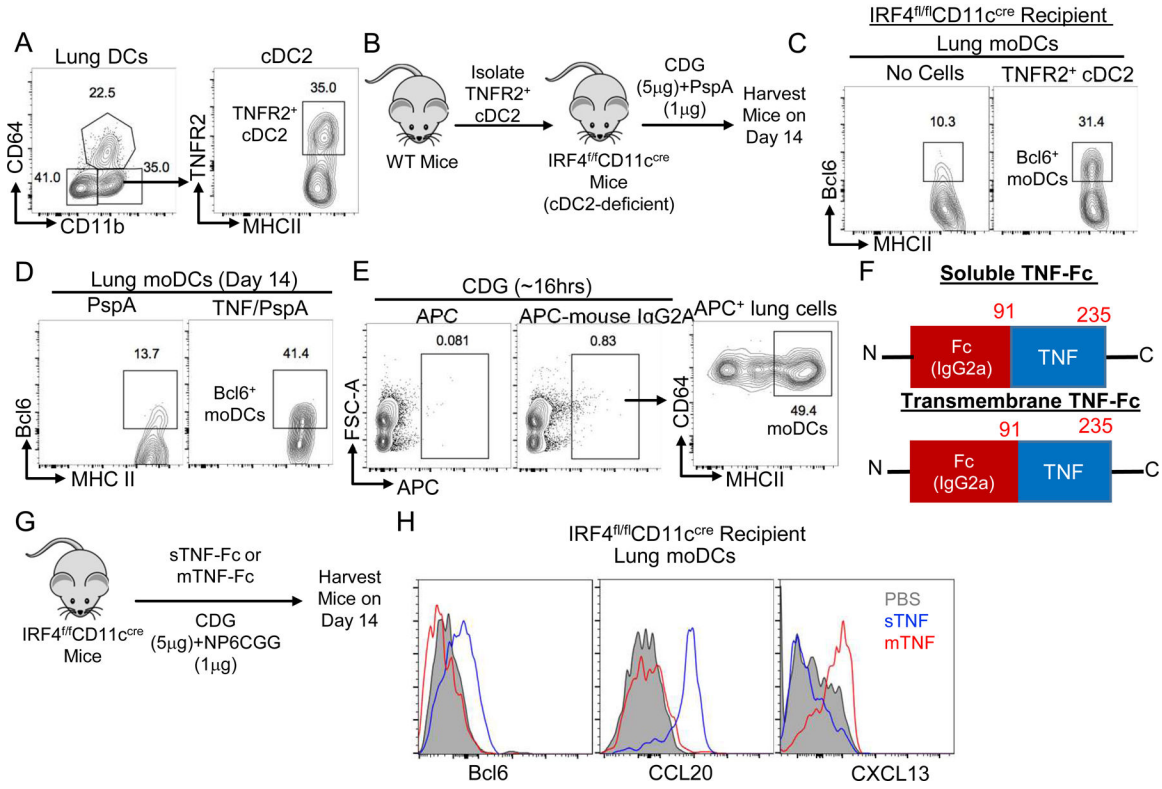

Figure 8. TNFR2$^+$ cDC2 produce soluble TNF to generate lung Bcl6$^+$ moDCs *in vivo*.

A. Gating strategy for the identification of TNFR2$^+$ cDC2 in the lung of naïve WT mice. **B.** Experimental design for TNFR2$^+$ cDC2 adoptive transfer. Lung TNFR2$^+$ cDC2 were isolated from the lungs of naïve WT mice. TNFR2$^+$ cDC2 (~50,000 cells) were intranasally transferred into IRF4$^{fl/fl}$CD11c^{cre} mice. Recipient IRF4$^{fl/fl}$CD11c^{cre} mice were immunized with CDG (5μg) and PspA (1μg). Mice were harvested on day 14. **C.** Flow cytometry analysis of Bcl6 expression on moDCs in IRF4$^{fl/fl}$CD11c^{cre} mice receiving TNFR2$^+$ cDC2 (n=3 mice/group). Data are representative of two independent experiments. **D.** WT mice were treated (*i.n.*) with 200ng recombinant TNF and PspA or PspA alone. On day 14, Bcl6$^+$ moDCs in the lung were determined by flow cytometry (n=3 mice/group). Data are representative of two independent experiments. **E.** C57BL/6J mice were administered (*i.n.*) with CDG/APC-mouse IgG2a (clone: MOPC-173) or CDG/APC only. Flow cytometry analysis of APC$^+$ cells were done in the lungs 16 hours post-treatment (n=3 mice/group). Data are representative of three independent experiments. **F.** Cartoon illustrating the sTNF-Fc (IgG2A) and tmTNF-Fc (IgG2A) fusion proteins. **G.** IRF4$^{fl/fl}$CD11c^{cre} mice were immunized (*i.n.*) with CDG/NP$_6$CGG and 100ng tmTNF-Fc (IgG2A) or 100ng sTNF-Fc (IgG2A). Lungs were harvested on day 14. **H.** Flow cytometry analysis of Bcl6, CCL20, and CXCL13 expression by lung moDCs from immunized mice. (n=3 mice/group). Data are representative of three independent experiments.

Table 1.

Lung DC subsets and CDG vaccine responses in various genetically modified mouse strains[1]

Mouse Strains	Lung moDCs	Lung cDC1	Lung cDC2	Lung Mucosal CDG Response	Systemic CDG Response
$CCR2^{-/-}$	Reduced in numbers	Normal	Normal	No IgA No Memory T_H cells	Normal
$Batf3^{-/-}$ [25]	Normal	Depleted	Normal	Normal	Normal
$IRF4^{fl/fl}CD11c^{cre}$ [25]	Normal	Normal	Depleted	No IgA No Memory T_H cells	No Serum IgG No Spleen memory T_H cells
$RelA^{fl/fl}CD11c^{cre}$	No activation by CDG	Normal	Normal	No IgA No Memory T_H cells	Normal
$Bcl6^{fl/fl}CD11c^{cre}$	Increased in numbers	Depleted	Constitutively activated	Has IgA No Memory T_H cells	Normal
$Bcl6^{fl/fl}LysM^{cre}$	Reduced in numbers	Normal	Normal	No IgA No Memory T_H cells	Normal

[1]Examining lung moDCs, cDC1 and cDC2 populations and their responses to CDG adjuvant *in vivo*.